Supplementary Fig.1.

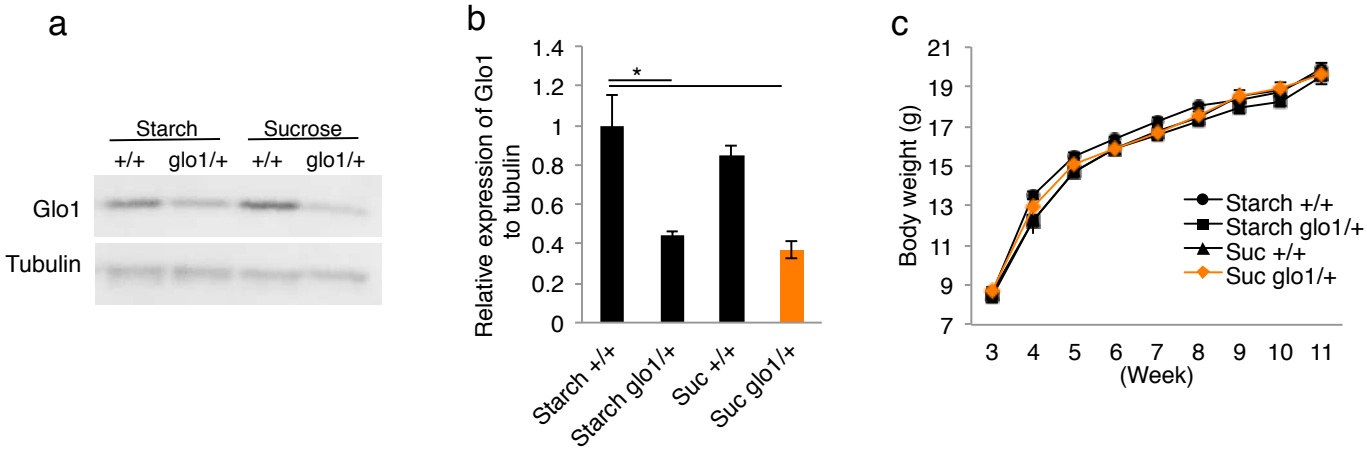

Supplementary Figure 1 Characterization of Glo1 expression level and mice in the four groups.
(a) Western blot analysis of the GLO1 protein using tubulin as an internal control. The cerebral cortex, including the hippocampus, was used as the loading sample. **(b)** Densitometric analysis of the expression levels of the GLO1 protein (Starch +/+, n = 3; Starch *Glo1*/+, n = 4; Suc +/+, n = 3; Suc *Glo*1/+, n = 4). To evaluate the expression levels of GLO1, the intensities of bands shown in a were divided by their corresponding intensities in the control (tubulin). **(c)** Body weight trajectories. No significant differences were observed among the groups (n = 9–10 mice per group). The statistical tests used included Dunnett's test in **b** and two-way repeated-measures ANOVA in c; main effect of group ($F_{3, 33} = 1.7512$, $P = 0.1757$). The data are presented as the mean ± s.e.m. *$P < 0.05$.

Supplementary Fig.2.

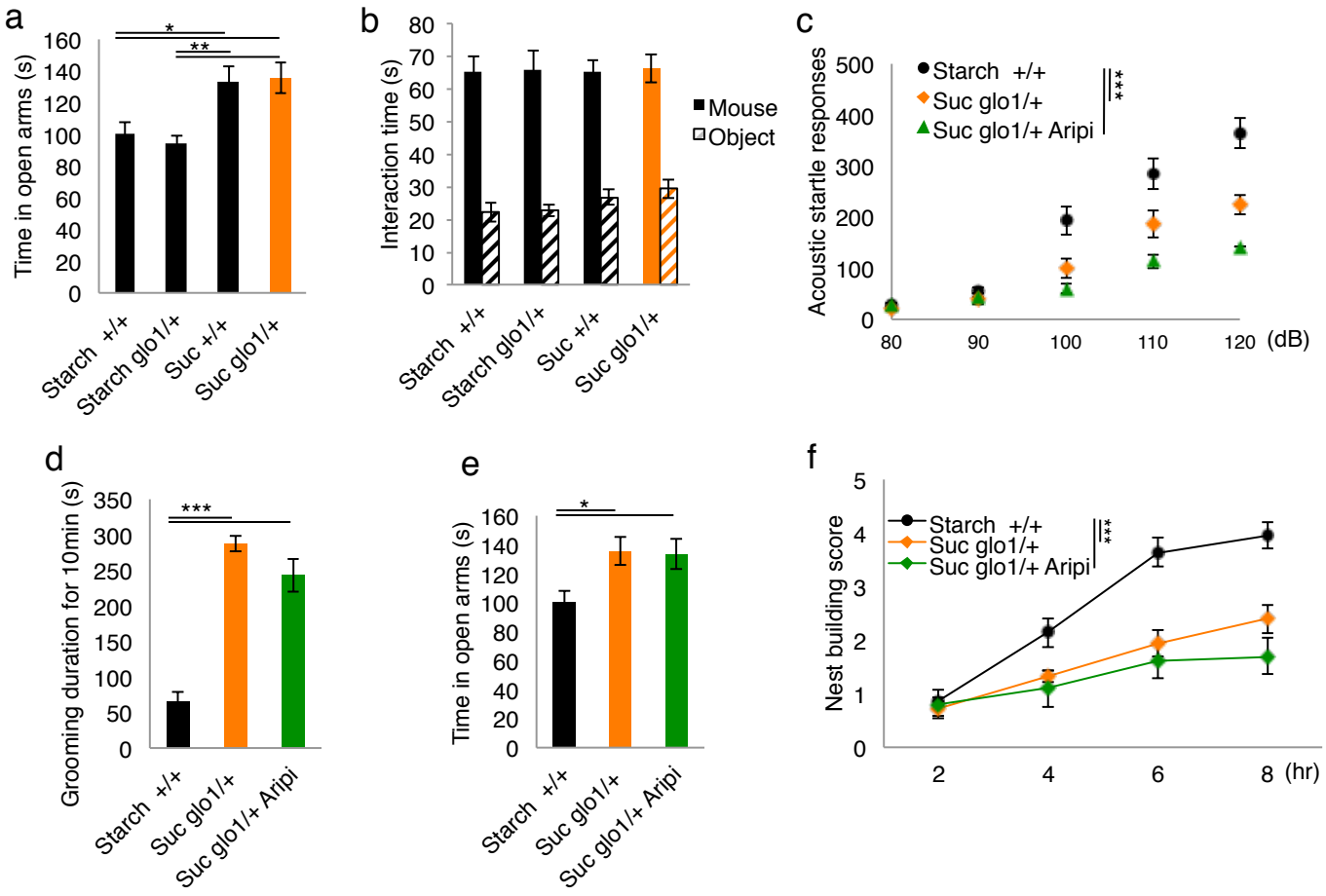

Supplementary Figure 2 Behavioral phenotypes and the effect of aripiprazole treatment.
(a) Elevated plus-maze test (to evaluate anxiety). **(b)** Interaction time with an empty cylinder (object) or a mouse placed in the cylinder in the social interaction test. No differences were detected in the social interaction test among the four groups. **(c–f)** Effects of aripiprazole treatment on the acoustic startle response **(c)**, self-grooming **(d)**, elevated plus-maze test **(e)**, and nest-building skills **(f)**. The abnormal behaviors of G×E mice in these tests were not improved by aripiprazole treatment. The statistical tests used included the Tukey–Kramer test in **a**,**b**,**d**, and **e**; and two-way repeated-measures ANOVA in **c** and **f**; main effect of group in **c** ($F2, 35 = 8.557$, $P = 0.0009$) and **f** ($F2, 47 = 14.6637$, $P = 0.004$). The data are presented as the mean ± s.e.m. *$P < 0.05$; **$P < 0.01$; ***$P < 0.001$.

Supplementary Fig.3.

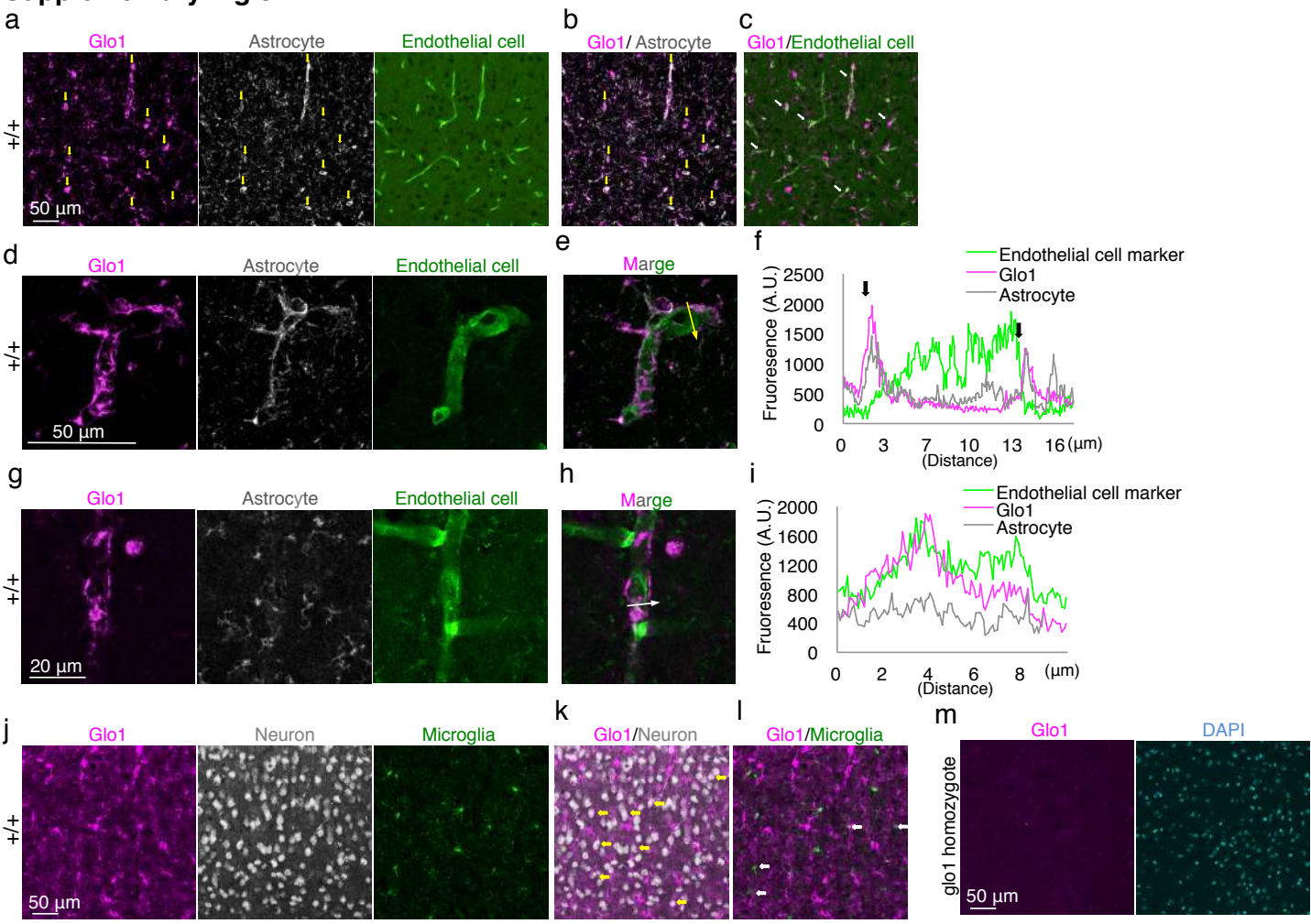

Supplementary Figure 3 Investigation of GLO1 localization in the cerebral cortices in sucrose-fed wild-type mice. **(a–f)** Localization of GLO1 in astrocytes. **(a)** Immunohistological images of GLO1 coimmunostaining with an astrocyte marker (ALDH1L1) or with an endothelial cell marker (tomato-lectin). **(b)** Merged image of GLO1 and ALDH1L1 in a. The yellow arrows in b indicate cells with colocalization of GLO1 and ALDH1L1. **(c)** Merged image of GLO1 and lectin in a. The white arrows point to the representative GLO1-positive cells located close to the endothelial cells. **(d,e)** Higher-magnification images of GLO1 coimmunostaining with ALDH1L1 or with tomato-lectin from a different focal plane. **(e)** Merged image of GLO1 and ALDH1L1 in d. **(f)** Plots of pixel intensities along the yellow arrow in e. The black arrows indicate the areas of colocalization of GLO1 and ALDH1L1. **(h)** Merged image of GLO1 and tomato-lectin in **g**. **(i)** Plots of pixel intensities along the white arrow in h. Unlike that observed in f, the GLO1 expression pattern showed a similar tendency to that of tomato-lectin expression, while ALDH1L1 exhibited a different expression pattern. **(j)** Coimmunostaining of GLO1 with the neuronal marker NeuN and the microglial marker IBA1. **(k)** Merged image of GLO1 and NeuN in j. The yellow arrows indicate neurons with mild GLO1 immunoreactivity. **(l)** Merged image of GLO1 and IBA1 in j. The white arrows indicate microglia with weak GLO1 immunoreactivity. **(m)** GLO1 immunostaining together with DAPI staining in *Glo1* homozygous mice.

Supplementary Fig.4.

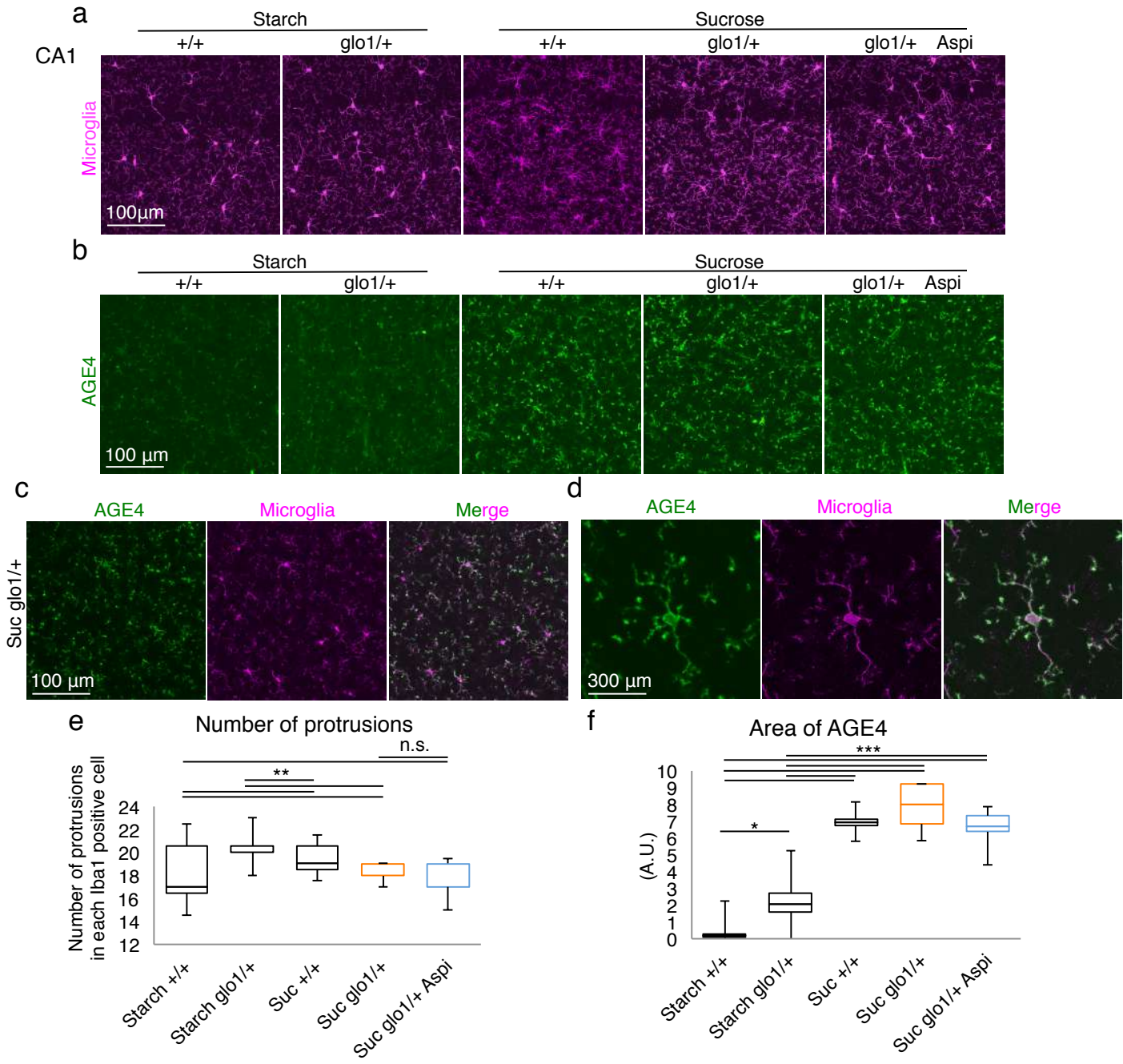

Supplementary Figure 4 Fructose-derived AGE accumulation in microglia in sucrose-fed mice.
(a,b) Immunohistochemical images of the microglial marker (IBA1) and AGE4 in the CA1 region. **(c)** Merged image of AGE4 and IBA1. **(d)** Higher-magnification images of AGE4 coimmunostaining with IBA1. **(e)** Number of protrusions in each IBA1-positive cell in each image in a. Mean number of protrusions in five randomly selected cells per image from three independent mice. **(f)** Measurement of the area covered with AGEs in a, in which the area is above the appropriate threshold of pixel intensity in each image. The mean intensity of the entire image was measured for each section (n = 4–5 slices per group). The statistical tests used included the Tukey–Kramer test in **e** and **f**. *$P < 0.05$; **$P < 0.01$; ***$P < 0.001$.

Supplementary Fig.5.

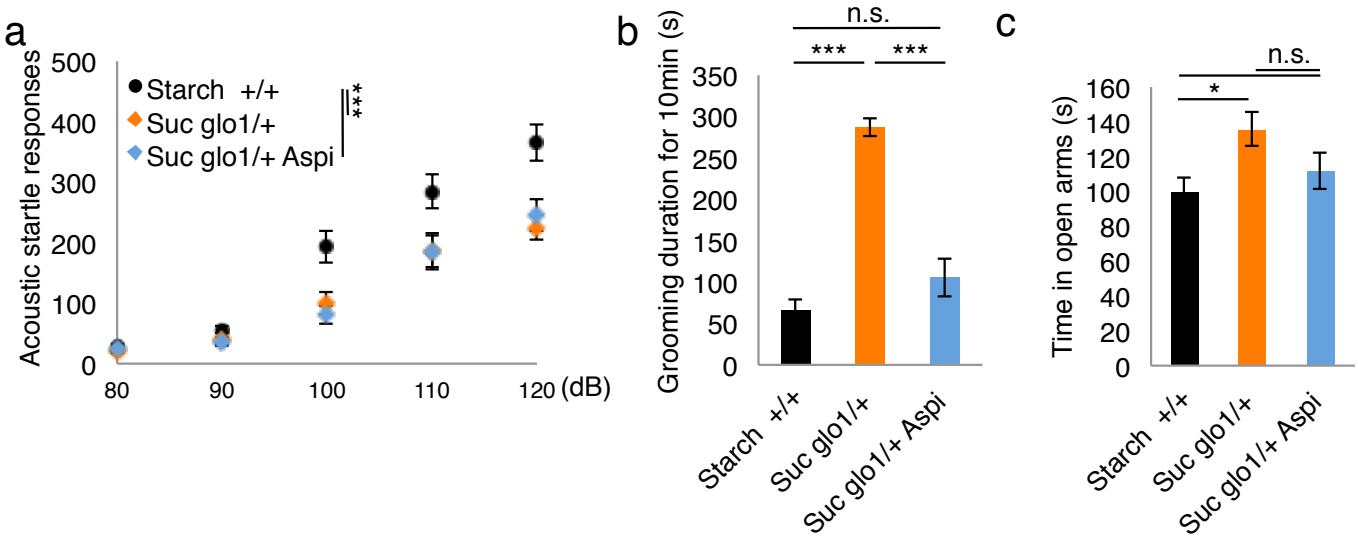

Supplementary Figure 5 Protective effects of aspirin against the development of abnormal behaviors in G×E mice.
(a–c) Effects of aspirin treatment on the acoustic startle response **(a)**, self-grooming **(b)**, and elevated plus-maze **(c)** tests. The administration of aspirin led to effective prevention of deficits in grooming duration and partially ameliorated the decline in acoustic responses; it also improved the time spent in the open arms in the elevated plus-maze test in G×E mice. The statistical tests used included two-way repeated-measures ANOVA in **a** ($F2, 42 = 8.0903$, $P = 0.0011$) and the Tukey–Kramer test in **b** and **c**. The data are presented as the mean ± s.e.m. *$P < 0.05$; ***$P < 0.001$.